THE ASTROPHYSICAL JOURNAL, 630:1213–1216, 2005 September 10

MEASUREMENT OF ABSOLUTE CROSS SECTIONS FOR EXCITATION OF THE $2s^2\ ^1S \rightarrow 2s2p\ ^1P^o$ TRANSITION IN O^{+4}

S. J. SMITH,[1] N. DJURIĆ,[1] J. A. LOZANO,[1] K. A. BERRINGTON,[2] AND A. CHUTJIAN[1]
Received 2004 December 29; accepted 2005 May 4

ABSTRACT

Experimental cross sections are reported for the $1s^22s^2\ ^1S \rightarrow 1s^22s2p\ ^1P^o$ transition in O^{+4} located at 19.689 eV. Use is made of the electron energy-loss method, using a merged electron-ion beam geometry. The center-of-mass interaction energies for the measurements in the $^1S \rightarrow {}^1P^o$ transition are in the range 18 eV (below the threshold) to 30 eV. Data are compared with other previous electron energy-loss measurements and with results of a 26 term ***R***-matrix calculation that includes fine structure explicitly via the Breit-Pauli Hamiltonian. Clear resonance enhancement is observed in all experimental and theoretical results near the threshold for this $^1S \rightarrow {}^1P^o$ transition.

Subject headings: atomic data — atomic processes — stars: abundances — Sun: abundances

1. INTRODUCTION

Transitions excited by electron impact in the O^{+4} ion have been detected in the lower solar transition region (Doschek et al. 2004), in the transition region of the stars Capella (Linsky et al. 1995) and AU Mic (Del Zanna et al. 2002), and in circumstellar regions (Kaspi et al. 2004). Discrepancies in the use of transitions in O^{+4} as diagnostics of electron density N_e have been noted by Dufton et al. (1978) and Pagano et al. (2004) and may arise from the choice of the atomic calculation for the effective collision strengths (Berrington 1994). In this regard, a number of collision strength calculations exist for highly charged ions (HCIs) using the ***R***-matrix approach (Berrington et al. 1977, 1979, 1981, 1985; Widing et al. 1982; Bannister et al. 1999). Comparisons have been made in the Be-like ions between tokamak-observed line emission intensities and intensities predicted from distorted wave and ***R***-matrix theories (Finkenthal et al. 1987). There are very few experimental measurements to verify the results of the theoretical calculations. Uncertainties in these results can arise from, for example, the different approximations to the electron + HCI Hamiltonian; the choice of target wave functions, continuum orbitals, and pseudostates; the number of partial waves included; and relativistic effects. There is an analogous requirement of an experimental method. The experimental approach should access both spin- and symmetry-allowed and -forbidden transitions. It should cover the excitation threshold region (where excitation cross sections are at a maximum, and where electron energy distribution functions in many astronomical plasmas have a maximum) and be able to attain higher energies in order to connect with distorted wave and Born approximations. The beam should be free of (or corrected for) metastable levels, and signals should also be free of (or corrected for) the underlying and often more intense elastic (Rutherford) electron-ion scattering. The electron energy-loss approach meets many of these requirements. It has been applied successfully to electron ion excitation using crossed electron and ion beams (Chutjian & Newell 1982) and merged beams (Smith et al. 1991; Wåhlin et al. 1991). Reported in the present study are new Jet Propulsion Laboratory (JPL) merged beam measurements of absolute excitation cross sections for the $1s^22s^2\ ^1S \rightarrow 1s^22s2p\ ^1P^o$ transition in O^{+4} at 19.689 eV. Comparison is made with theoretical results in a 26 state ***R***-matrix calculation and with a separate energy loss/merged beam measurement of a different geometry (Bannister et al. 1999).

2. EXPERIMENTAL METHODS

Measurements were carried out using the 14.0 GHz electron cyclotron resonance ion source (ECRIS) at JPL, and details are given in Chutjian et al. (1999) and Greenwood et al. (1999). The $^{18}O^{+4}$ ions were generated from $^{18}O_2$ feed gas and extracted from the ECRIS at an energy of 4×7.0 keV. The metastable fraction in the beam was determined using the gas attenuation method (Greenwood et al. 2000). Other procedures, such as measurements of the electron and ion beam overlap, use of the electrostatic mirror, use of the electrostatic aperture, use of a retarding-grid electric field along the solenoidal axis to discriminate against elastically scattered electrons, and correction above the threshold for overlap between high-angle elastically scattered electrons and low-angle inelastically scattered electrons, have been given in Smith et al. (2000).

The relation between the measured experimental quantities and the absolute excitation cross section $\sigma(E)$ (in units of square centimeters) at a center-of-mass (CM) energy E is given by

$$\sigma(E) = \frac{\mathfrak{R} q e^2 F}{\varepsilon I_i I_e L}\left|\frac{v_e v_i}{v_e - v_i}\right|, \quad (1)$$

where $\mathfrak{R}$ is the total signal rate (in units of inverse seconds), q (= 4 here) is the ionic charge state, e is the electron charge (in units of coulombs), I_e and I_i are the electron and ion beam currents (in units of amperes), respectively, v_e and v_i are the electron and ion velocities (in units of centimeters per second), respectively, L is the merged path length (in units of centimeters), ε is the combined efficiency of the retarding grid/microchannel plate detection system (dimensionless), and F is the overlap factor between the electron and ion beams (in units of square centimeters). The quantities in equation (1) are measured, with the exception of the velocities v_e and v_i, which are known nominally through their acceleration potentials.

Results of theoretical calculations for these transitions were obtained from a 26 LS-coupled target state ***R***-matrix calculation including the fine structure explicitly via the Breit-Pauli Hamiltonian. This calculation is a refinement over the six-state

[1] Jet Propulsion Laboratory, California Institute of Technology, Pasadena, CA 91109.
[2] School of Science and Mathematics, Sheffield Hallam University, Sheffield S1 1WB, UK.

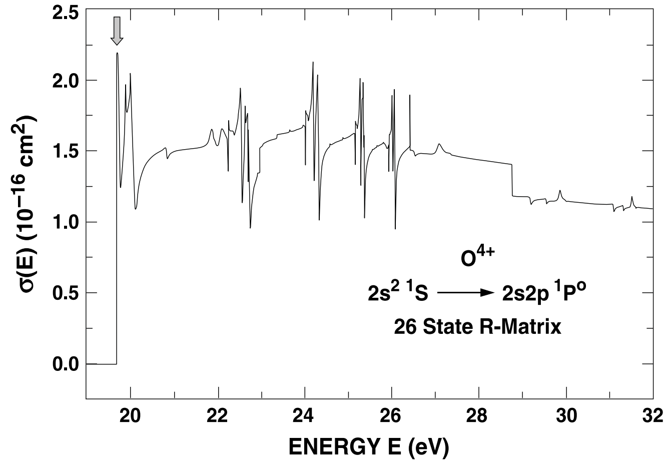

FIG. 1.—Absolute cross sections for the $2s^2\ ^1S \rightarrow 2s2p\ ^1P^o$ transition in O^{+4} calculated in the 26 state ***R***-matrix theory. Results are not convoluted with any experimental parameters and show the marked resonance enhancement of the cross section in this threshold region. The theoretical curve was shifted by 0.08 eV to lower energies to agree with the spectroscopic threshold of 19.689 eV (indicated by the arrow).

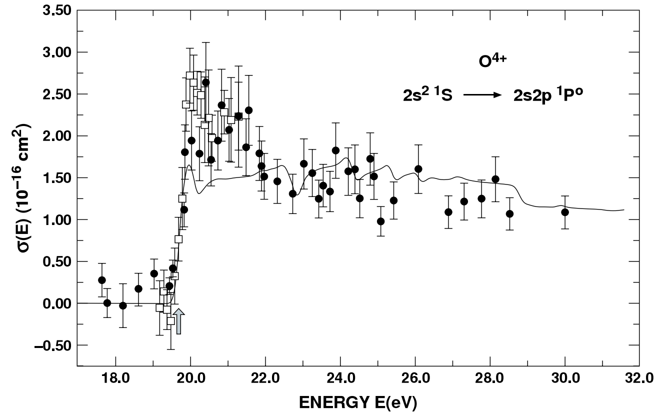

FIG. 2.—Comparison of the present, experimental absolute excitation cross sections for the $2s^2\ ^1S \rightarrow 2s2p\ ^1P^o$ transition in O^{+4} (*filled circles*) with theoretical results of a 26 term ***R***-matrix calculation (*solid line*). Experimental results are given at the 1.7 σ (90%) confidence level, and theoretical results have been convoluted with a 0.20 eV experimental energy resolution. Also shown are experimental energy-loss results of Bannister et al. (1999; *open squares*, with only the relative uncertainties shown). The arrow indicates the energy onset for this transition at 19.689 eV.

R-matrix results previously reported in Bannister et al. (1999). It includes all the $2l2l'$ and $2l3l'$ terms, where l refers to an s or p electron and l' refers to an s, p, or d electron. Two correlation pseudoorbitals of the type $\overline{4d}$ and $\overline{4f}$ were also introduced into the target configuration interaction expansion to improve the representation of the $2s2p\ ^1P^o$ and $2p^2\ ^1D$ terms. The standard Breit-Pauli ***R***-matrix programs of Berrington et al. (1995) were then used.

Results of the calculations in just the threshold region (19.689–22 eV) are shown in Figure 1. One sees that from theory alone, the excitation cross sections for this resonance transition are dominated by a large number of sharp resonances, most of them having widths smaller than the energy resolution of the present experiment (0.20 eV, or 1.53×10^{-2} ryd). In order to compare experiment and calculation on an equal resolution footing, the theoretical cross section results were convoluted with an energy-dependent width ΔE in the CM frame given by (Smith et al. 2000)

$$\Delta E = \Delta E_e \left[1 - \left(\frac{m_e}{m_i} \right)^{1/2} \left(\frac{E_i}{E_e} \right)^{1/2} \cos \vartheta \right]. \quad (2)$$

Here, ΔE_e is the electron energy width (FWHM) in the laboratory frame, m_i and m_e are the electron and ion masses, E_e and E_i are the electron and ion laboratory-frame energies, and ϑ is the laboratory-frame angle between the merged electron and ion beams (hence $\vartheta \approx 0°$). Using values appropriate for $^{18}O^{+4}$, one obtains the CM width ΔE as a function of laboratory-frame width ΔE_e by

$$\Delta E = \Delta E_e \left[1 - 5.5007 \times 10^{-3} \left(\frac{E_i}{E_e} \right)^{1/2} \right]. \quad (3)$$

The widths from equation (3) were calculated for $\Delta E_e = 0.25$ eV (which includes the combined effect of the electron gun energy spread and beam broadening by the trochoidal monochromator) and an ion beam energy $E_i = 28.0$ keV.

Results of the present experiment and those of Bannister et al. (1999) are presented in Figure 2. The present uncertainty limits represent a total quadrature uncertainty in the measurements of 20% at the 1.7 σ level, and approximately 25% of the data involve two measurements at a given energy. A list of the components of this total uncertainty can be found in Niimura et al. (2002). Also shown in Figure 2 are results of the 26 term ***R***-matrix calculation, as convoluted with a $\Delta E = 0.20$ eV energy broadening in the measurements. The agreement between the present data and calculation at energies above 22 eV is very good. At energies from the threshold (19.689 eV) to 22 eV, both the present experimental results and those of Bannister et al. (1999) lie 15%–65% higher than theory predicts. As noted by Bannister et al. (1999), some of the previous discrepancy between experiment and theory could have arisen through the value adopted by Bannister et al. (1999), for a different type of electron cyclotron resonance (ECR) ion source, of a metastable fraction of 0.42.

In the present work, the beam attenuation method was used to determine the metastable fraction (Liao et al. 1997). The attenuating gases used were He, N_2, and Ar, with most of the data taken using Ar. In all cases a break in the slope of O^{+4} beam attenuation versus gas pressure was observed. As another check on the technique, no break was found with the ions H^+ (no metastable levels possible) and H_2^+ (none observed experimentally). A total of 19 attenuation measurements were made during the course of the cross section measurements. The total range of metastable fractions measured was 10%–42%, with 14 of the 19 measured fractions being less than or equal to 25%. The estimated statistical uncertainty in each fraction was 8% and included uncertainties in the measurement of the attenuation slopes, intercept, attenuating gas pressure, and counting statistics of the transmitted O^{+4} beam current. Within the total experimental uncertainty there was no systematic dependence of cross section on the applied metastable fraction.

The metastable fraction in the ECR ion source can be varied. In previous lifetime measurements using trapped metastable ions, this fraction was adjusted—by varying the ECR gas pressure, microwave power, and strength of the solenoidal magnetic field—to give an optimum signal of metastable photon emission (Smith et al. 2004). Hence, by measuring the metastable fraction under actual source operating conditions, one source of experimental uncertainty in the present excitation measurements has been reduced. Nevertheless, as also noted by Bannister et al.

TABLE 1

Experimental Cross Sections $\sigma(E)$ and Collision Strengths $\Omega(E)$ for the $2s^2\ {}^1S \rightarrow 2s2p\ {}^1P^o$ Resonance Transition in O^{+4}

Energy E (eV)	Energy E (ryd)	Experimental $\sigma(E)$ (10^{-16} cm^2)	Experimental Collision Strength $\Omega(E)$ (dimensionless)
17.6	1.296	0.28	0.41
17.8	1.306	0.01	0.01
18.2	1.336	−0.02	−0.04
18.6	1.366	0.18	0.28
19.0	1.397	0.36	0.58
19.4	1.427	0.21	0.34
19.5	1.433	0.42	0.69
19.8_0	1.455	1.13	1.87
19.8_2	1.456	1.82	3.01
20.0	1.470	1.96	3.28
20.2	1.485	1.80	3.04
20.4	1.498	2.65	4.51
20.5	1.508	1.73	2.97
20.7	1.521	1.96	3.39
20.8	1.529	2.38	4.14
21.0	1.544	2.09	3.67
21.3	1.562	2.25	3.99
21.4	1.577	1.88	3.37
21.5	1.582	2.32	4.17
21.8	1.602	1.80	3.28
21.8_6	1.607	1.65	3.01
21.9_3	1.612	1.53	2.80
22.3	1.638	1.47	2.74
22.7	1.668	1.32	2.50
23.0	1.691	1.68	3.23
23.2	1.707	1.57	3.05
23.4	1.720	1.26	2.46
23.5	1.729	1.42	2.79
23.7	1.742	1.35	2.67
23.9	1.754	1.84	3.67
24.2	1.778	1.59	3.21
24.4	1.791	1.62	3.30
24.5	1.801	1.27	2.60
24.8	1.821	1.74	3.60
24.9	1.829	1.53	3.18
25.1	1.842	0.99	2.07
25.4	1.867	1.24	2.63
26.1	1.916	1.62	3.53
26.9	1.976	1.10	2.47
27.3	2.007	1.23	2.81
27.8	2.041	1.26	2.92
28.1	2.068	1.49	3.50
28.5	2.096	1.08	2.57
30.0	2.205	1.09	2.73

Note.—Nonzero values below the threshold include effects of the electron energy spread in the experiment.

(1999), the calculated cross sections in the threshold region remain 15%–65% smaller than experimental ones.

All experimental data are listed in Table 1. Also listed are the corresponding values of the dimensionless collision strength $\Omega(E)$ defined by

$$\Omega(E) = \frac{\sigma(E)}{\pi a_0^2}\omega_i \frac{E}{I_H}. \qquad (4)$$

Here, ω_i is the statistical weight of the ground ^1S state ($\omega_i = 1$), E is the CM energy (in units of eV), I_H is the Rydberg unit of energy (13.6058 eV), and a_0 is the Bohr radius (0.5292×10^{-8} cm). The

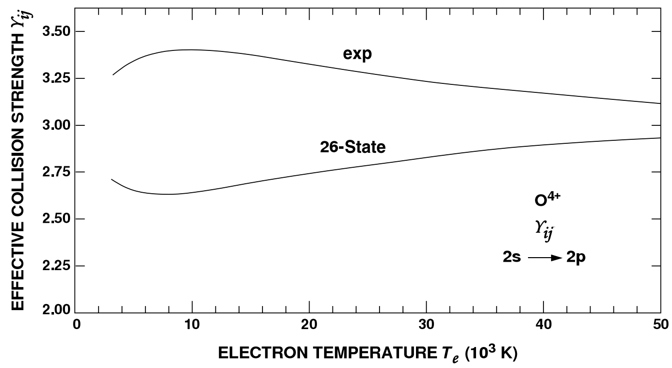

Fig. 3.—Variation of the effective collision strength Υ_{ij} with electron temperature T_e from equation (5). The experimental strengths and results from the 26 state calculation are shown. The total quadrature uncertainty in the experimental Υ_{ij} is 20% (1.7σ).

thermally averaged (effective) collision strength Υ_{ij} and excitation rate C_{ij} are derived by integrating over the energy-dependent collision strength Ω_{ij} as

$$\Upsilon_{ij} = \int_0^\infty \Omega_{ij}(E) \exp\left(-E_j/kT\right) d\left(E_j/kT\right), \qquad (5)$$

$$C_{ij}(T_e) = \left(\frac{8.63 \times 10^{-6}}{T_e^{1/2}\omega_i}\right) \exp\left(-\frac{E_{ij}}{kT_e}\right) \Upsilon_{ij}(T_e)\ \mathrm{cm}^3\ \mathrm{s}^{-1}, \qquad (6)$$

where T_e is the temperature (in units of kelvins), E_{ij} is the energy difference (in units of rydbergs) between the target levels, E_j is the energy (in units of rydbergs) of the electron after excitation (with the target in the final state j), and k is the Boltzmann constant (in units of rydbergs per kelvin). Results for Υ_{ij} from equation (5) are shown in Figure 3, where the integration was done using the calculated collision strengths Ω_{ij} and the experimental collision strengths in Table 1. Since the theory and experiment essentially converge above 50,000 K, one may conclude that the existing collision strength data in the literature (which are based on theory) should be valid for higher temperatures, for example, for the peak of the ionization balance in stellar atmospheres at 250,000 K.

One may also see from Figure 3 that the experimental strengths are about 25% (at the threshold) to 5% higher than the theoretical results, which is a reflection of the higher experimental cross sections (Fig. 1). The difference in shapes versus T_e of the data is also a reflection of the slightly different appearance of the resonance structure in the experiment versus the theoretical calculations.

Measurements of absolute collision cross sections at and above the threshold provide an important benchmark for theoretical results. Such measurements must be made for the important ionic emitters in the solar, stellar, and interstellar regions (Chutjian 2004). Experimental-theoretical comparisons are critical in evaluating the success of theory to calculate the vast majority of cross sections. Results such as those of Figure 3 give a clear representation of the utility of a particular theory for calculating excitation rates.

N. Djurić and J. Lozano thank the National Research Council for support. This work was carried out at the Jet Propulsion Laboratory, California Institute of Technology, and was supported under contract with the National Aeronautics and Space Administration.

REFERENCES

Bannister, M. E., Djurić, N., Woitke, O., Dunn, G. H., Chung, Y.-S., Smith, A. C. H., Wallbank, B., & Berrington, K. A. 1999, Int. J. Mass Spectrom., 192, 39
Berrington, K. A. 1994, At. Data Nucl. Data Tables, 57, 71
Berrington, K. A., Burke, P. G., Dufton, P. L., & Kingston, A. E. 1977, J. Phys. B, 10, 1465
———. 1981, At. Data Nucl. Data Tables, 26, 1
———. 1985, At. Data Nucl. Data Tables, 33, 195
Berrington, K. A., Burke, P. G., Dufton, P. L., Kingston, A. E., & Sinfailam, A. L. 1979, J. Phys. B, 12, L275
Berrington, K. A., Eissner, W. B., & Norrington, P. H. 1995, Comput. Phys. Commun., 92, 290
Chutjian, A. 2004, Phys. Scr., T110, 203
Chutjian, A., Greenwood, B. J., & Smith, S. J. 1999, in AIP Conf. Proc. 475, Applications of Accelerators in Research and Industry, ed. J. L. Duggan & I. L. Morgan (Woodbury: AIP), 881
Chutjian, A., & Newell, W. R. 1982, Phys. Rev. A, 26, 2271
Del Zanna, G., Landini, M., & Mason, H. E. 2002, A&A, 385, 968
Doschek, G. A., Mariska, J. T., & Akiyama, S. 2004, ApJ, 609, 1153
Dufton, P. L., Berrington, K. A., Burke, P. G., & Kingston, A. E. 1978, A&A, 62, 111
Finkenthal, M., et al. 1987, ApJ, 313, 920
Greenwood, J. B., Chutjian, A., & Smith, S. J. 2000, ApJ, 529, 605
Greenwood, J. B., Smith, S. J., Chutjian, A., & Pollack, E. 1999, Phys. Rev. A, 59, 1348
Kaspi, S., Netzer, H., Chelouche, D., George, I. M., Nandra, K., & Turner, T. J. 2004, ApJ, 611, 68
Liao, C., Smith, S. J., Hitz, D., Chutjian, A., & Tayal, S. S. 1997, ApJ, 484, 979
Linsky, J. L., Wood, B. E., Judge, P., Brown, A., Andrulis, C., & Ayres, T. R. 1995, ApJ, 442, 381
Niimura, M., Čadež, I., Smith, S. J., & Chutjian, A. 2002, Phys. Rev. Lett., 88, 103201
Pagano, I., Linsky, J. L., Valenti, J., & Duncan, D. K. 2004, A&A, 415, 331
Smith, S. J., Čadež, I., Chutjian, A., & Niimura, M. 2004, ApJ, 602, 1075
Smith, S. J., Greenwood, J. B., Chutjian, A., & Tayal, S. S. 2000, ApJ, 541, 501
Smith, S. J., Man, K.-F., Mawhorter, R. J., Williams, I. D., & Chutjian, A. 1991, Phys. Rev. Lett., 67, 30
Wåhlin, E. K., Thompson, J. S., Dunn, G. H., Phaneuf, R. A., Gregory, D. C., & Smith, A. C. H. 1991, Phys. Rev. Lett., 66, 157
Widing, K. G., Doyle, J. G., Dufton, P. L., & Kingston, A. E. 1982, ApJ, 257, 913